Title

Gas-Phase Structure Determination of Dihydroxycarbene, One of the Smallest Stable Singlet Carbenes

Permalink

https://escholarship.org/uc/item/2c158264

Journal

Angewandte Chemie International Edition, 53(16)

ISSN

1433-7851

Authors

Womack, Caroline C
Crabtree, Kyle N
McCaslin, Laura
et al.

Publication Date

2014-04-14

DOI

10.1002/anie.201311082

Copyright Information

Peer reviewed

Gas-phase structure determination of dihydroxycarbene, one of the smallest stable singlet carbenes

Caroline C. Womack[1], Kyle N. Crabtree[2], Laura McCaslin[3], Oscar Martinez Jr.[2], Robert W. Field[1], John F. Stanton[3], Michael C. McCarthy[2]*

[1]*Department of Chemistry, Massachusetts Institute of Technology, Cambridge, MA 02139*
[2]*Harvard-Smithsonian Center for Astrophysics, Cambridge, MA, 02138*
[3]*Department of Chemistry & Biochemistry, University of Texas at Austin, Austin, TX, 78712*
*Corresponding author. Email: mmccarthy@cfa.harvard.edu.

Abstract: Carbenes are reactive molecules of the form R_1-$\ddot{C}$-R_2 that play a role in topics ranging from organic synthesis to gas-phase oxidation chemistry. We report the first experimental structure determination of dihydroxycarbene (HO-$\ddot{C}$-OH), one of the smallest stable singlet carbenes, using a combination of microwave rotational spectroscopy and high-level coupled-cluster calculations. The semi-experimental equilibrium structure derived from five isotopic variants of HO-$\ddot{C}$-OH contains two very short CO single bonds ($\sim$1.32 Å). Detection of HO-$\ddot{C}$-OH in the gas phase firmly establishes that it is a stable molecule, yet it has been underrepresented in discussions of the CH_2O_2 chemical system and its atmospherically relevant isomers: formic acid and the Criegee intermediate CH_2OO.

Carbenes (R_1-$\ddot{C}$-R_2) comprise an important class of molecules in chemistry owing to a highly reactive electron-deficient carbon atom. Relatively stable singlet carbenes with bulky electron-donating substituents, such as N-heterocyclic carbenes, have long been used in organic synthesis [1, 2], but smaller carbenes are more difficult to isolate and characterize. Numerous studies [3–7] implicate small organic carbenes as intermediates in chemical reactions such as the thermal decomposition of dicarboxylic acids (which are a key component of secondary organic aerosols [8–10], photochemical smog [11], and interstellar clouds [12]) and the reactions of carbon dioxide and carbon monoxide with H_2O/H_2, thought to be important in prebiotic chemistry [12–14] and in reversible hydrogen storage [15, 16]. Although triatomic carbenes (:CX_2 where X = H, F, Cl, Br, or I) and vinylidene (:C=CH_2) have been studied extensively [17–22], fewer experimental studies have examined the properties of small carbenes with substituent groups containting two to three atoms, which have a larger range

of possible reaction pathways [23–29].

It is understood that carbenes are stabilized by nearby electron-donating groups [1]. Several groups have calculated the potential energy surface (PES) of one of the smallest carbenes with two electron-donating groups: the singlet ground state of dihydroxycarbene (HO-C̈-OH) [3, 4, 23], which has been suggested to be an intermediate in the photolysis of oxalic acid [30, 31]. The three local minima of the singlet HO-C̈-OH PES, shown below, are some
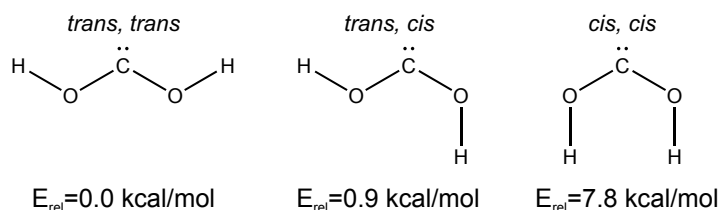
of the most thermodynamically stable isomers of the CH_2O_2 family, lying approximately 167 kJ/mol higher than formic acid, but roughly 335 kJ/mol *lower* than the recently detected Criegee intermediate [32–35], CH_2OO, and 250 kJ/mol lower than dioxirane [4], yet are rarely considered in the literature. The stability of singlet HO-C̈-OH is provided by the overlap between the electrons in the oxygen p orbitals and the empty p orbital on the carbon, leading to much shorter CO bond lengths (1.32 Å) [4, 23] than those found in alcohols (such as the 1.42 Å CO bond length in methanol [36]). The triplet state lacks an empty p orbital and is stabilized to a much lesser extent by this overlap and so lies nearly 125 kJ/mol higher in energy, in contrast to many other carbenes [3].

The first experimental evidence for the existence of dihydroxycarbene was inferred by neutralization/reionization mass spectroscopy (NRMS) [24, 25]. More recently, Schreiner *et al.* reported the generation of *trans, trans*- and *trans, cis*-HO-C̈-OH via the thermal extrusion of CO_2 from oxalic acid and its subsequent isolation in an argon matrix at 10 K [23]. A similar experiment showed that hydroxycarbene (H-C̈-OH) rapidly isomerizes to formaldehyde (CH_2O) at 10 K, a phenomenon attributed to quantum tunneling through the

125 kJ/mol barrier [6, 26]. In contrast, HO-C̈-OH displays no tunneling behavior and is stable under the low-temperature matrix conditions. Subsequent work with several substituted oxycarbenes indicates that the propensity for tunneling is greatly influenced by the identity of the substituent [7, 27, 37, 38].

We present here the first direct gas phase evidence for *trans, cis*-HO-C̈-OH, and a precise determination of its rotational spectrum and geometric structure, using a combination of Fourier transform microwave spectroscopy (FTMW), microwave-millimeter wave double resonance (DR) spectroscopy, and high-level theoretical calculations. The 5-43 GHz Balle-Flygare type FTMW spectrometer used in these experiments has been described elsewhere [39–42], so only a brief description is provided here; a more extensive discussion can be found in the Supporting Documents. A gaseous mixture of 0.5% CO_2 and 12.5% H_2 in Ne was supersonically expanded into a Fabry-Pérot cavity through a pulsed valve coupled to a DC electrical discharge source, which produced *trans, cis*-HO-C̈-OH in detectable yield. (The *trans, trans*- and *cis, cis*- isomers may also be present, but both only possess b-type rotational transitions, which lie above the frequency ceiling of our spectrometer (see Supporting Documents), and were therefore not measured in this work.) Four isotopic variants of HO-C̈-OH were detected under similar conditions using an appropriate isotopically-enriched precursor gas analog ($C^{18}O_2$, $^{13}CO_2$, or an H_2/D_2 mixture). A short microwave pulse (1 μs) excited the rotational transitions that fell within the narrow bandwidth of the cavity ($\sim$1 MHz). A Fourier transform of the free induction decay (FID) emitted by the coherently rotating molecules yielded a power spectrum. The lines with frequencies >40 GHz were detected using microwave-millimeter wave double resonance spectroscopy, a technique that is used to confirm assignments and extend measurements to higher frequencies [42–45]. Sample FTMW and DR spectra are shown in Figure 1. In total, at least four $J_{K_a,K_c} - J'_{K'_a,K'_c}$ rotational transitions were measured (see Table 1) for HO-C̈-OH and four of its isotopologues: HO-^{13}C̈-OH, H^{18}O-C̈-^{18}OH, HO-C̈-OD$_{cis}$ and D$_{trans}$O-C̈-OH.

The SPFIT/SPCAT suite of programs was used to derive the molecular constants, A_0, B_0, and C_0, from a least squares fit to the experimentally measured transitions [46]. The vibrationally corrected, semi-experimental equilibrium rotational constants, A_e^{SE}, B_e^{SE}, and C_e^{SE}, were determined for each species (see Table 2) and used to determine a semi-experimental equilibrium structure (r_e^{SE}, shown in Figure 2) using the STRFIT program [47]. Several theoretical studies have confirmed a planar structure of dihydroxycarbene [3, 4, 23] and the derived inertial defects (Δ in Table 2) are uniformly small for all isotopic species, indicating that the molecule is planar and does not undergo large amplitude motions [48]. All structural parameters have estimated 1σ uncertainties less than 0.5% of their respective values, and are in excellent agreement with recent calculations [4, 23], including the CCSD(T)/cc-pCVQZ ab initio structure calculated in this work using the electronic structure package in the CFOUR suite of programs (see Figure 2) [49–51].

The PES calculated by Schreiner et $al.$ [23] suggests that HO-C̈-OH, with sufficient internal energy, may surmount one of the $\sim$138 kJ/mol barriers to form formic acid or dissociate to CO_2 + H_2 or CO + H_2O [23]. Their measurement of the HO-C̈-OH lifetime at 10 K demonstrates that it is not susceptible to quantum tunneling, unlike H-C̈-OH and CH_3-C̈-OH. From our relative intensity measurements, we conclude that HO-C̈-OH is present at 7% of the level of $trans$-formic acid, indicating that the lifetime of HO-C̈-OH in the gas phase is at least a few ms and that its abundance is sizable. The structure in Figure 2 contains two very short C-O single bonds, lending further credence to the assertion that the substantial overlap between the oxygen and carbon p orbitals is the root cause of the molecule's stability [3, 23]. These results illustrate the critical role that the second electron-donating group plays in quenching tunneling to formic acid. Exploring the behavior of other electron-donating substituents (such as nitrogen-containing groups) and performing more detailed lifetime measurements would help to answer questions about how this quenching is achieved.

The close agreement between the theoretical predictions and the experimental results, and the certainty with which the structural parameters are determined leaves little doubt about the identity and structure of *trans, cis*-HO-C̈-OH. Experimental evidence for the apparent gas-phase stability of this carbene indicates that HO-C̈-OH should be included in discussions of the reactivity of the CH_2O_2 isomeric family, which includes the simplest Criegee intermediate and formic acid. Although CH_2OO was not present in our CO_2/H_2 discharge source, we have recently generated CH_2OO in a CH_4/O_2 mixture [52] in comparable abundance to HO-C̈-OH. One of the established unimolecular reactions of vibrationally excited CH_2OO is isomerization to the more stable formic acid isomer [34]; HO-C̈-OH is usually not considered in those discussions despite its relative thermodynamic stability. Taatjes *et al.* found that the Criegee intermediates, CH_2OO and CH_3CHOO, will readily donate a weakly bound oxygen to the common atmospheric oxides NO_2 and SO_2 and postulated that Criegee intermediates may play an important role in nitrate and sulfate chemistry [33, 53, 54]. Given the reactive nature of its carbon atom, yet its relative stability to unimolecular dissociation, HO-C̈-OH formed under atmospheric conditions could play a similarly important role, albeit one involving reactions of the electron-deficient carbon atom with hydrocarbons. HO-C̈-OH could also be formed by the hydrogenation of HOCO, a radical species with numerous applications in atmospheric and combustion chemistry [55]. However, further study of this molecule must be undertaken to fully understand its reactivity and its role in atmospheric processes.

Acknowledgements

References

[1] H. W. Wanzlick, *Angew. Chem. Int. Ed. Engl.* **1962**, *1*, 75–80.

[2] A. J. Arduengo III, R. L. Harlow, M. Kline, *J. Am. Chem. Soc.* **1991**, *113*, 361–3.

[3] D. Feller, W. T. Borden, E. R. Davidson, *J. Chem. Phys.* **1979**, *71*, 4987–92.

[4] S.-W. Hu, S.-M. Lü, X.-Y. Wang, *J. Phys. Chem. A* **2004**, *108*, 8485–94.

[5] D. L. Reid, J. Hernández-Trujillo, J. Warkentin, *J. Phys. Chem. A* **2000**, *104*, 3398–405.

[6] L. Koziol, Y. Wang, B. J. Braams, J. M. Bowman, A. I. Krylov, *J. Chem. Phys.* **2008**, *128*, 204310–9.

[7] V. G. Kiselev, S. Swinnen, V. S. Nguyen, N. P. Gritsan, M. T. Nguyen, *J. Phys. Chem. A* **2010**, *114*, 5573–9.

[8] M. Z. H. Rozaini in *Atmospheric Aerosols - Regional Characteristics - Chemistry and Physics*, (Ed. H. Abdul-Razzak), InTech, **2012**, pg. 329.

[9] K. Kawamura, E. Tachibana, K. Okuzawa, S. G. Aggarwal, Y. Kanaya, Z. F. Wang, *Atmos. Chem. Phys.* **2013**, *13*, 8285–302.

[10] V.-M. Kerminen, C. Ojanen, T. Pakkanen, R. Hillamo, M. Aurela, J. Meriläinen, *J. Aerosol Sci.* **2000**, *31*, 349–62.

[11] W. F. Rogge, M. A. Mazurek, L. M. Hildemann, G. R. Cass, B. R. T. Simoneit, *Atmos. Environ. A - Gen.* **1993**, *27*, 1309–30.

[12] V. Blagojevic, S. Petrie, D. K. Bohme, *Mon. Not. R. Astron. Soc.* **2003**, *339*, L7–L11.

[13] E. C. C. Baly, I. M. Heilbron, W. F. Barker, *J. Chem. Soc., Trans.* **1921**, *119*, 1025–35.

[14] K. Ruiz-Mirazo, C. Briones, A. de la Escosura, *Chem. Rev.* **2013**, (in press).

[15] S. Enthaler, J. von Langermann, T. Schmidt, *Energy Environ. Sci.* **2010**, *3*, 1207–17.

[16] K. Schuchmann, V. Müller, *Science* **2013**, *342*, 1382–5.

[17] G. Herzberg, J. Shoosmith, *Nature* **1959**, *183*, 1801–2.

[18] R. L. Schwartz, G. E. Davico, T. M. Ramond, W. C. Lineberger, *J. Phys. Chem. A* **1999**, *103*, 8213–21.

[19] N. Hansen, H. Mäder, F. Temps, *Phys. Chem. Chem. Phys.* **2001**, *3*, 50–5.

[20] O. Suto, J. Steinfeld, *Chem. Phys. Lett.* **1990**, *168*, 181–4.

[21] K. K. Murray, D. G. Leopold, T. M. Miller, W. C. Lineberger, *J. Chem. Phys.* **1988**, *89*, 5442–53.

[22] K. M. Ervin, J. Ho, W. C. Lineberger, *J. Chem. Phys.* **1989**, *91*, 5974–92.

[23] P. R. Schreiner, H. P. Reisenauer, *Angew. Chem. Int. Ed.* **2008**, *47*, 7071–4.

[24] F. A. Wiedmann, J. Cai, C. Wesdemiotis, *Rapid Commun. Mass Spectrom.* **1994**, *8*, 804–7.

[25] P. C. Burgers, G. A. McGibbon, J. K. Terlouw, *Chem. Phys. Lett.* **1994**, *224*, 539–43.

[26] P. R. Schreiner, H. P. Reisenauer, F. C. Pickard IV, A. C. Simmonett, W. D. Allen, E. Mátyus, A. G. Császár, *Nature* **2008**, *453*, 906–9.

[27] P. R. Schreiner, H. P. Reisenauer, D. Ley, D. Gerbig, C.-H. Wu, W. D. Allen, *Science* **2011**, *332*, 1300–3.

[28] E. P. Clifford, P. G. Wenthold, W. C. Lineberger, G. A. Petersson, G. B. Ellison, *J. Phys. Chem. A* **1997**, *101*, 4338–45.

[29] R. R. Lucchese, H. F. Schaefer III, *J. Am. Chem. Soc.* **1977**, *99*, 13–4.

[30] T. Kakumoto, K. Saito, A. Imamura, *J. Phys. Chem.* **1987**, *91*, 2366–71.

[31] S. Yamamoto, R. A. Back, *J. Phys. Chem.* **1985**, *89*, 622–5.

[32] R. Criegee, *Angew. Chem. Int. Ed. Engl.* **1975**, *14*, 745–52.

[33] O. Welz, J. D. Savee, D. L. Osborn, S. S. Vasu, C. J. Percival, D. E. Shallcross, C. A. Taatjes, *Science* **2012**, *335*, 204–7.

[34] Y.-T. Su, Y.-H. Huang, H. A. Witek, Y.-P. Lee, *Science* **2013**, *340*, 174–6.

[35] J. M. Beames, F. Liu, L. Lu, M. I. Lester, *J. Am. Chem. Soc.* **2012**, *134*, 20045–8.

[36] R. M. Lees, F. J. Lovas, W. H. Kirchhoff, D. R. Johnson, *J. Phys. Chem. Ref. Data* **1973**, *2*, 205–14.

[37] D. Gerbig, D. Ley, H. P. Reisenauer, P. R. Schreiner, *Beilstein J. Org. Chem.* **2010**, *6*, 1061–9.

[38] D. Gerbig, H. P. Reisenauer, C.-H. Wu, D. Ley, W. D. Allen, P. R. Schreiner, *J. Am. Chem. Soc.* **2010**, *132*, 7273–5.

[39] T. J. Balle, W. H. Flygare, *Rev. Sci. Instrum.* **1981**, *52*, 33–45.

[40] M. C. McCarthy, M. J. Travers, A. Kovács, C. A. Gottlieb, P. Thaddeus, *Astrophys. J. Suppl. Ser.* **1997**, *113*, 105–20.

[41] M. C. McCarthy, W. Chen, M. J. Travers, P. Thaddeus, *Astrophys. J. Suppl. Ser.* **2000**, *129*, 611–23.

[42] M. C. McCarthy, V. Lattanzi, D. Kokkin, O. Martinez Jr., J. F. Stanton, *J. Chem. Phys.* **2012**, *136*, 034303–10.

[43] M. Nakajima, Y. Sumiyoshi, Y. Endo, *Rev. Sci. Instrum.* **2002**, *73*, 165–71.

[44] M. Nakajima, Y. Endo, *J. Chem. Phys.* **2013**, *139*, 101103–4.

[45] K. Suma, Y. Sumiyoshi, Y. Endo, *Science* **2005**, *308*, 1885–6.

[46] H. M. Pickett, *J. Mol. Spectrosc.* **1991**, *148*, 371–7.

[47] Z. Kisiel, *J. Mol. Spectrosc.* **2003**, *218*, 58–67.

[48] T. Oka, *J. Mol. Struct.* **1995**, *352-353*, 225–33.

[49] CFOUR, Coupled-Cluster Techniques for Computational Chemistry, a quantum-chemical program package by J. F. Stanton, J. Gauss, M. E. Harding, P. G. Szalay, with contributions from A. A. Auer, *et al.* For detailed information, see www.cfour.de.

[50] K. Raghavachari, G. W. Trucks, J. A. Pople, M. Head-Gordon, *Chem. Phys. Lett.* **1989**, *157*, 479–83.

[51] D. E. Woon, T. H. Dunning Jr., *J. Chem. Phys.* **1995**, *103*, 4572–85.

[52] M. C. McCarthy, L. Cheng, K. N. Crabtree, O. Martinez Jr., T. L. Nguyen, C. C. Womack, J. F. Stanton, *J. Phys. Chem. Lett.* **2013**, *4*, 4133–9.

[53] C. A. Taatjes, O. Welz, A. J. Eskola, *et al.*, *Science* **2013**, *340*, 177–80.

[54] C. J. Percival, O. Welz, A. J. Eskola, *et al.*, *Faraday Discuss.* **2013**, (preprint).

[55] J. S. Francisco, J. T. Muckerman, H.-G. Yu, *Acc. Chem. Res.* **2010**, *43*, 1519–26.

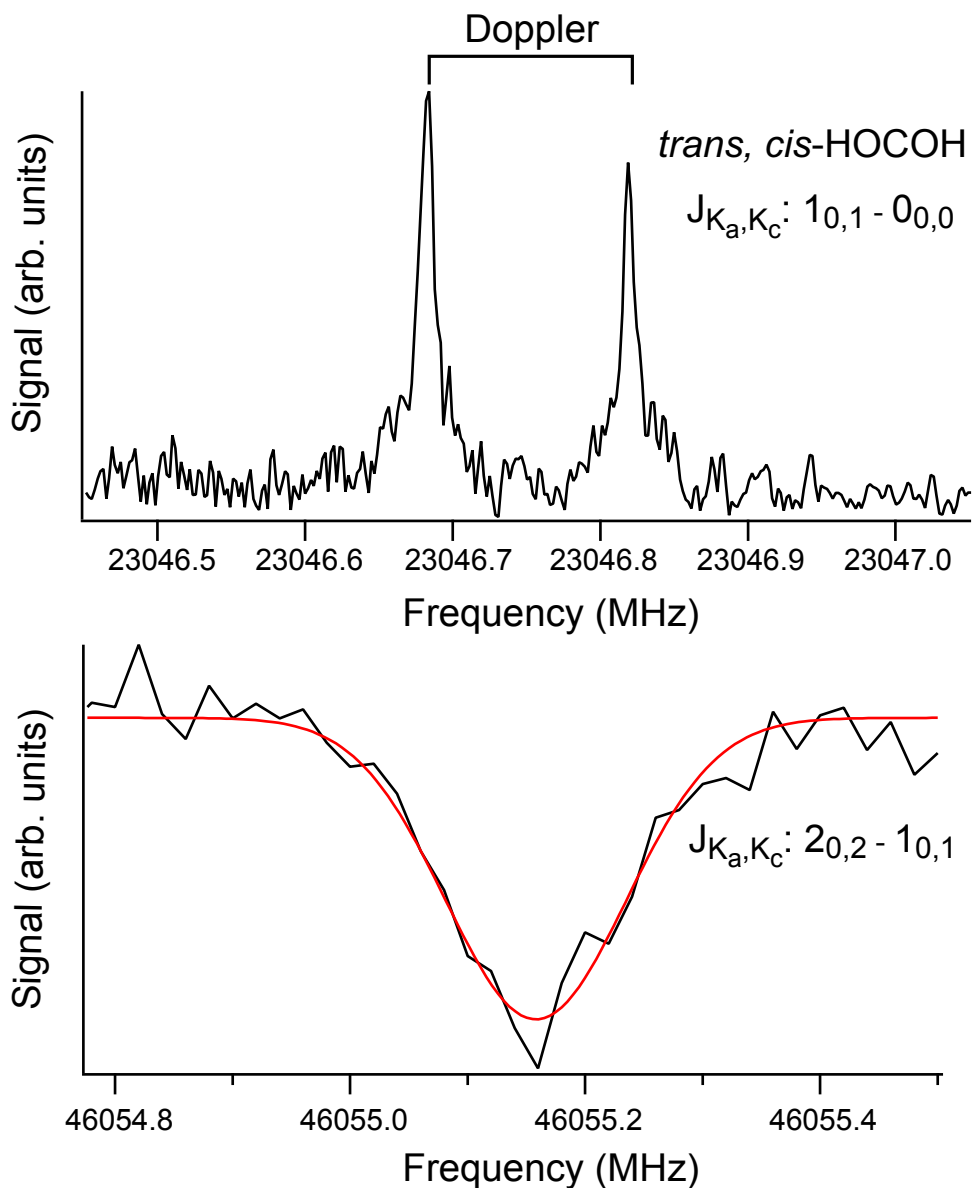[56] L. McCaslin, J. Stanton, *Mol. Phys.* **2013**, *111*, 1492–6.

Figure 1: A FTMW spectrum of the $1_{0,1} - 0_{0,0}$ transition (top frame) and DR spectrum of the $2_{0,2} - 1_{0,1}$ transition (bottom frame) of *trans, cis*-HO-C̈-OH. Two Doppler-split peaks appear in the FTMW spectrum because the molecular beam is aligned along the Fabry-Pérot cavity axis [39]. The DR spectrum was obtained by monitoring the intensity of the $1_{0,1} - 0_{0,0}$ spectrum as a second microwave synthesizer is swept in frequency near that predicted for the $2_{0,2} - 1_{0,1}$ transition. The depletion signal is fit to a Gaussian curve, shown in red, to determine the center frequency.
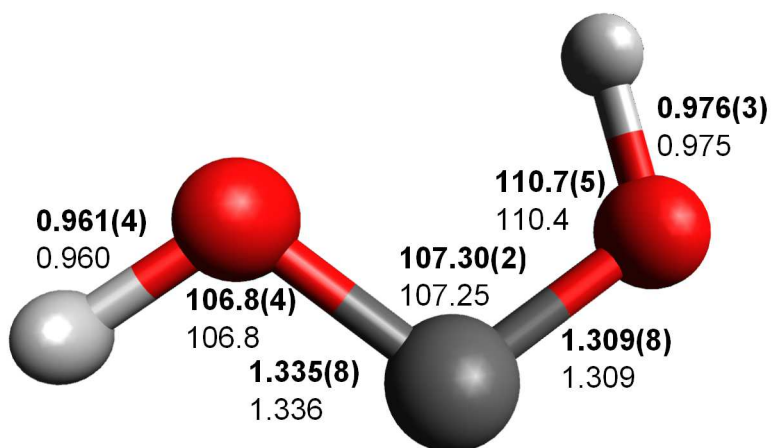
Figure 2: The semi-experimental equilibrium structure, r_e^{SE} of *trans, cis*-HO-C̈-OH. Bold numbers indicate semi-experimental values with estimated 1σ uncertainties given in parenthesis in the unit of the last digit. Normal script values show the ab initio structure, calculated at the CCSD(T)/cc-pCVQZ level of theory. The bond lengths are in Å and the bond angles are in degrees.

Transition	HO-C̈-OH	HO-^{13}C̈-OH	H^{18}O-C̈-^{18}OH	HO-C̈-OD$_{cis}$	D$_{trans}$O-C̈-OH
$1_{1,1} - 2_{0,2}$	16084.6005(20)	12686.6853(20)	20151.8988(20)	–	–
$1_{0,1} - 0_{0,0}$	23046.7507(20)	22973.2378(20)	20832.5530(20)	22415.1500(20)	21407.0360(20)
$2_{0,2} - 1_{0,1}$	46055.1580(100)	45902.3957(100)	41638.0770(100)	44773.8440(100)	42784.8405(250)
$1_{1,0} - 1_{0,1}$	63929.0101(100)	60454.4531(100)	63285.3450(100)	53336.5897(250)	63740.3755(250)
$1_{1,1} - 0_{0,0}$	85186.4955(100)	81562.2895(100)	82622.5246(100)	73772.1960(250)	83585.1815(250)

Table 1: Measured frequencies for several low-J transitions of isotopologues of HO-C̈-OH. All values are given in MHz, and the estimated 1σ uncertainties are given in parentheses in the unit of the last digit. The signal-to-noise ratio of the $1_{1,1} - 2_{0,2}$ transitions of the two singly deuterated species was too low to determine an exact frequency.

Constant	HO-C̈-OH	HO-^{13}C̈-OH	H^{18}O-C̈-^{18}OH	HO-C̈-OD$_{cis}$	D$_{trans}$O-C̈-OH
	Uncorrected values				
A_0	74559.0428(34)	71009.5742(75)	72955.1706(7)	63555.148(36)	73663.9592(70)
B_0	12418.0239(33)	12419.3332(73)	11163.9796(7)	12197.379(35)	11484.6541(70)
C_0	10628.7693(34)	10553.9479(76)	9668.6086(7)	10217.807(35)	9922.4236(70)
	Zero-point vibrational corrections				
ΔA	341.3648	304.6495	326.3149	374.4679	331.3751
ΔB	114.2458	112.9567	100.6500	103.2054	100.7534
ΔC	107.7056	105.6664	95.5990	98.6285	95.1602
	Semi-experimental rotational constants				
A_e^{SE}	74900.4076(34)	71314.2237(75)	73281.4855(7)	63929.616(36)	73995.3343(70)
B_e^{SE}	12532.2697(33)	12532.2899(73)	11264.6295(7)	12300.584(35)	11585.4075(70)
C_e^{SE}	10736.4749(34)	10659.6143(76)	9764.2077(7)	10316.436(35)	10017.5838(70)
Δ	-0.00234	-0.00217	-0.00232	-0.00326	-0.00272
	Ab initio rotational constants				
A_e	74833.7616	71247.2243	73213.5345	63906.8188	73931.6234
B_e	12532.3542	12532.3303	11264.3359	12303.2298	11586.5264
C_e	10734.6332	10657.6569	9762.3418	10317.0159	10016.7123

Table 2: ==A summary of rotational constants derived from the experimental data and theoretical calculations. All values shown in MHz unless otherwise stated. The estimated 1σ uncertainties are given in parentheses in the unit of the last digit. The uncorrected values were derived from a fit to the experimental transitions in== Table 1. Additional constants were used in the fitting procedure (see Table S1). The zero-point vibrational corrections were calculated at the CCSD(T)/ANO1 level [56], and the vibrationally corrected semi-experimental rotational constants were calculated as $A_e^{SE} = A_0 + \Delta A$. The inertial defect is defined as $\Delta = I_C - I_B - I_A$ and has units ==u==·Å^2. The rotational constants of the CCSD(T)/cc-pCVQZ ab initio structure, A_e, B_e and C_e, are shown here for comparison.

Supporting Documents for: Gas-phase structure determination of dihydroxycarbene, one of the smallest stable singlet carbenes

S1 Experimental methods

A gaseous mixture of CO_2 and H_2 diluted in Ne was supersonically expanded through a 6 Hz pulsed valve coupled to a DC-current electrical discharge source, which consists of two copper electrodes separated by Teflon spacers. Electrical discharges have previously been shown to readily generate a wide range of reactive species [1, 2], and here produces HO-C̈-OH in good yield. The supersonic expansion through the 1 mm pinhole results in the cooling of the molecules to $T_{\rm rot} = 1 - 3$ K. The entire discharge assembly is seated inside one of the two large aluminum mirrors, which together comprise a Fabry-Perot cavity and are located inside a large vacuum chamber typically held at a base pressure of ∼1×10^{-5} Pa. A short microwave pulse (1 μs) excites the rotational transitions that fall within the narrow bandwidth of the cavity (∼1 MHz). The free induction decay (FID) emitted by the coherently rotating molecules is detected by a heterodyne receiver and the Fourier transform yields the power spectrum. The molecular beam and the cavity axis are coaxial and thus two peaks are observed in the FT spectrum, owing to the Doppler effect.

Experimental conditions were initially optimized for the fundamental rotational transition $(1_{0,1} - 0_{0,0};$ 22471.18 MHz) of *trans*-formic acid [3], the most stable isomer of CH_2O_2 [4]. Under these conditions, the formic acid line was observed with good signal to noise. Once the fundamental line of dihydroxycarbene was found, conditions were then tuned to maximize the S/N of this peak. The normal HO-C̈-OH species was thus detected using a mixture of 0.5% CO_2 and 12.5% H_2 balanced in neon with a backing pressure of 333 kPa. The gas-pulse duration was 450 μs, resulting in a flow of 32 sccm (cubic centimeters per minute at stan-

, and the discharge voltage was $\sim$1.25 kV. The other isotopic species were detected under similar conditions in which an appropriate isotopically enriched precursor gas analog ($C^{18}O_2$, $^{13}CO_2$, or D_2) was used at the same concentrations. A mixture of H_2 and D_2 was used for the two singly deuterated species, HO-C̈-OD and DO-C̈-OH.

To guide the experimental work, an ab initio structure of dihydroxycarbene was calculated at the CCSD(T)/cc-pCVQZ level of theory [8, 9] using the electronic structure package in the CFOUR suite of programs [10]. Vibrational corrections to the rotational constants were calculated from the frozen core CCSD(T)/ANO1 quadratic and cubic force fields [11]. Analytic second derivatives were used, while the third geometrical derivatives were obtained via finite difference techniques.

For each isotopologue of HO-C̈-OH, the lowest two a-type transitions on the $K_a = 0$ ladder and the lowest two b-type transitions were detected. The fundamental a-type transition of the normal species was detected in a survey of the microwave region within 1.5% of the predicted frequency. A discharge-dependent line was soon found at 23046.75 MHz and was confirmed as the fundamental transition of HO-C̈-OH after subsequent detection of the isotopologues. The other lines were detected using microwave-millimeter wave double resonance, a technique that has been successfully used by our group and by others [2, 5–7]. In these experiments, the FT spectrometer is tuned to the $1_{0,1} - 0_{0,0}$ transition, and a second microwave synthesizer, aligned perpendicularly to the molecular beam axis, is swept in frequency near that predicted for the $2_{0,2} - 1_{0,1}$ transition. When the second frequency is resonant with this transition, a depletion in the intensity of the $1_{0,1} - 0_{0,0}$ line is observed. The depletion spectrum is fit by a Gaussian line profile to obtain the center frequency of the transition.

The *trans, cis*-HO-C̈-OH isomer measured here has a calculated dipole component of 1.70 Debye along the a axis, and 1.74 Debye along the b axis, which enables both a-type and b-type rotational transitions to be measured. Both *trans, trans*-HO-C̈-OH and *cis, cis*-HO-

C̈-OH have vanishingly small dipole components along their a axes, and thus only b-type transitions would have been observed for these conformers, which occur at frequencies outside the range of our spectrometer. Detection and structure determination of these conformers in a millimeter-wave spectrometer is certainly possible and could answer questions about steric hinderance experienced by the hydrogen atoms, but is left to future work.

S2   Mechansim of formation in the discharge source

Schreiner's PES shows that dihydroxycarbene can be formed by the concerted addition of H_2 to the oxygens in CO_2 [12]. The HO-C̈-OH molecules in our studies, however, appear to form via sequential addition of hydrogens: a mechanism that involves three molecules, which by definition could not be included in Schreiner's bimolecular PES. Evidence for this mechanism is provided by the existence of all four possible deuterated variants of dihydroxy-carbene in roughly equal amounts when an H_2/D_2 mixture is used. (Although DO-C̈-OD was not used in the structural analysis, its $1_{0,1} - 0_{0,0}$ transition was detected at 20818.97 MHz.) Only HO-C̈-OH and DO-C̈-OD would be generated in a concerted mechanism. Previous experiments have demonstrated that hydrogen atoms are readily generated from H_2 in an electric discharge [2], and we have also observed *trans*-HOCO radicals in our CO_2/H_2 plasma. The CO_2 in the discharge plasma likely reacts with either H· and D· atoms to form HOCO/DOCO, which then reacts with another hydrogen atom or dihydrogen molecule prior to supersonic expansion and cooling.

S3   Quadrupole splitting in the deuterated species

The spectra of the $1_{0,1} - 0_{0,0}$ transition of the deuterium-containing species, shown in Figure S1, exhibited splitting on the order of 30 kHz, which was attributed to quadrupole-quadrupole coupling. The major peak is attributed to the F $= 2 - 1$ transition, with weaker peaks on either side attributed to the F $= 1 - 1$ and $1 - 0$ transitions, although the latter

could not be seen in the DOCOH spectrum. All detected peaks were included in the least-squares fitting of the molecular constants and the resulting χ_{aa} parameter for both species is shown in Table S1. χ_{aa} is a measure of the extent to which the quadrupole moment is projected onto the a-axis, which lies along the OCO backbone. Although the error bars for these derived values are larger than those of the other values in Table S1, they are still roughly in line with what that would be expected for our structure. When the deuterium is in the *trans* position (DOCOH), χ_{aa} is nearly double in magnitude and opposite in sign to when it is in the *cis* position (HOCOD).

References

[1] Y. Endo, H. Kohguchi, Y. Ohshima, *Faraday Discuss.* **1994**, *97*, 341–50.

[2] M. C. McCarthy, V. Lattanzi, D. Kokkin, O. Martinez Jr., J. F. Stanton, *J. Chem. Phys.* **2012**, *136*, 034303–10.

[3] M. Winnewisser, B. P. Winnewisser, M. Stein, M. Birk, G. Wagner, G. Winnewisser, K. M. T. Yamada, S. P. Belov, O. I. Baskakov, *J. Mol. Spectrosc.* **2002**, *216*, 259–65.

[4] S.-W. Hu, S.-M. Lü, X.-Y. Wang, *J. Phys. Chem. A* **2004**, *108*, 8485–94.

[5] M. Nakajima, Y. Endo, *J. Chem. Phys.* **2013**, *139*, 101103–4.

[6] K. Suma, Y. Sumiyoshi, Y. Endo, *Science* **2005**, *308*, 1885–6.

[7] K. Suma, Y. Sumiyoshi, Y. Endo, *J. Chem. Phys.* **2004**, *121*, 8351–9.

[8] K. Raghavachari, G. W. Trucks, J. A. Pople, M. Head-Gordon, *Chem. Phys. Lett.* **1989**, *157*, 479–83.

[9] D. E. Woon, T. H. Dunning Jr., *J. Chem. Phys.* **1995**, *103*, 4572–85.

[10] CFOUR, Coupled-Cluster Techniques for Computational Chemistry, a quantum-chemical program package by J. F. Stanton, J. Gauss, M. E. Harding, P. G. Szalay, with contributions from A. A. Auer, *et al.* For detailed information, see www.cfour.de.

[11] L. McCaslin, J. Stanton, *Mol. Phys.* **2013**, *111*, 1492–6.

[12] P. R. Schreiner, H. P. Reisenauer, *Angew. Chem. Int. Ed.* **2008**, *47*, 7071–4.

S4   Additional Figures and Tables

Table S1: Distortion constants and χ parameters used in the structural fit of HO-C̈-OH. D_J, D_K and D_{JK} were calculated at the CCSD(T)/ANO1 level of theory and held constant, while χ_{aa} was optimized in the least-squares fitting procedure, along with the A_0, B_0 and C_0 rotational constants shown in Table 2. All values are in units of MHz. The estimated 1σ uncertainties are shown in parentheses in the unit of the last digit.

Constant	HO-C̈-OH	HO-^{13}C̈-OH	H^{18}O-C̈-^{18}OH	HO-C̈-OD$_{cis}$	D$_{trans}$O-C̈-OH
D_J	0.0107	0.0106	0.0087	0.0108	0.0084
D_K	1.3259	1.2308	1.2805	0.7548	1.2091
D_{JK}	-0.0312	-0.0284	-0.0318	-0.0113	-0.0212
χ_{aa}	–	–	–	-0.1331(113)	0.2322(56)

Table S2: Components of the dipole moment of the isotopologues of dihydroxycarbene, calculated at the CCSD(T)/ANO1 level of theory. All values are in units of Debye.

Constant	HO-C̈-OH	HO-^{13}C̈-OH	H^{18}O-C̈-^{18}OH	HO-C̈-OD$_{cis}$	D$_{trans}$O-C̈-OH
A	1.7049	1.7052	1.7132	1.6558	1.6787
B	-1.7431	-1.7428	-1.7350	-1.7898	-1.7683
C	0	0	0	0	0

Table S3: Components of the quadrupole moment of the isotopologues of dihydroxycarbene, calculated at the CCSD(T)/ANO1 level of theory. All values are in units of Debye.

Constant	HO-C̈-OH	HO-^{13}C̈-OH	H^{18}O-C̈-^{18}OH	HO-C̈-OD$_{cis}$	D$_{trans}$O-C̈-OH
AA	6.3235	6.28024	6.3054	6.9969	6.3122
AB	8.7362	8.6757	8.8522	8.4461	8.7463
AC	0	0	0	0	0
BB	-4.0671	-3.9813	-4.0941	-4.7588	-4.1605
BC	0	0	0	0	0
CC	-2.2565	-2.2988	-2.2113	-2.2381	-2.1517

Table S4: Cartesian coordinates of optimized *trans, cis*-HO-C̈-OH geometry at the CCSD(T)/cc-pCVQZ level of theory. Coordinate values are reported in Å. Masses are reported in u. The isotopologues were calculated with the following isotopic masses: ^{13}C = 13.00335483 u, ^{18}O = 17.99916030 u, and D = 2.014101779 u.

Atom	Mass	Coordinate		
		X	Y	Z
H_{trans}	1.0078	1.8261	0.3031	0
O	15.9949	1.0366	-0.2432	0
C	12.0000	-0.0088	0.5884	0
O	15.9949	-1.0909	-0.1484	0
H_{cis}	1.0078	-0.8581	-1.0949	0

Table S5: The harmonic frequencies of the normal modes of vibration of the ab initio equilibrium structure of *trans, cis*-HO-C̈-OH, calculated at the CCSD(T)/ANO1 level of theory. The second column, shown in italics, displays the harmonic frequencies of the normal species calculated at the CCSD(T)/cc-pVTZ level of theory by Schreiner *et al* [12]. All values are given in units of cm^{-1}.

| HO-C̈-OH	*HO-C̈-OH*	HO-^{13}C̈-OH	H^{18}O-C̈-^{18}OH	HO-C̈-OD$_{cis}$	D$_{trans}$O-C̈-OH
631.37	*634.2*	627.12	609.43	574.37	499.81
658.72	*658.1*	658.64	655.67	574.85	603.64
780.08	*789.8*	776.48	774.39	698.11	769.18
1115.48	*1133.5*	1101.66	1085.76	985.85	922.23
1171.27	*1181.6*	1161.90	1153.25	1145.24	1125.15
1335.57	*1353.3*	1318.75	1319.60	1245.14	1308.67
1431.90	*1440.5*	1410.36	1419.20	1400.60	1398.98
3599.31	*3607.5*	3599.27	3588.34	2616.31	2801.35
3847.65	*3865.6*	3847.63	3835.17	3847.45	3599.55
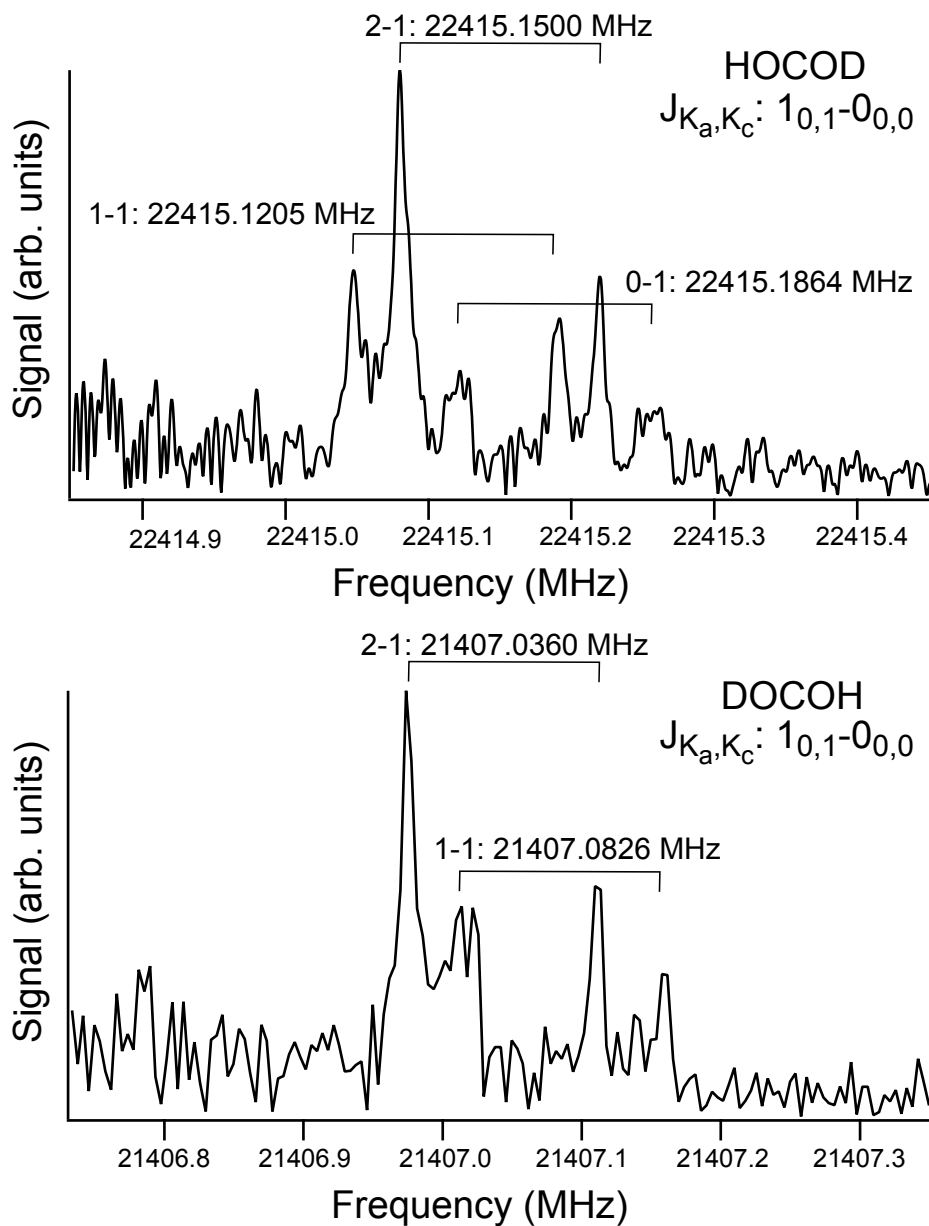
Figure S1: The FTMW spectra of the $1_{0,1} - 0_{0,0}$ transitions of both $HOCOD_{cis}$ (top) and $D_{trans}OCOH$ (bottom). Each spectrum exhibits splitting due to deuterium quadrupole coupling. Two sets of peaks are evident due to the Doppler effect and each Doppler pair is labeled with the F - F' quantum numbers of the transition and measured frequency.